Wind/SWE observations of firehose constraint on solar wind proton temperature anisotropy

Justin C. Kasper and Alan J. Lazarus
Center for Space Research, MIT, Cambridge, Massachusetts, USA

S. Peter Gary
Los Alamos National Laboratory, Los Alamos, New Mexico, USA

Received 14 March 2002; revised 29 April 2002; accepted 6 May 2002; published 12 September 2002.

[1] The proton resonant firehose instability may arise in collisionless plasmas in which the proton velocity distribution is approximately bi-Maxwellian with $T_{\|p}/T_{\perp p} > 1$, where $\perp$ and $\|$ denote directions relative to the background magnetic field $\mathbf{B}_\circ$. Linear theory and one-dimensional simulations predict that enhanced field fluctuations from the proton resonant firehose instability impose a constraint on proton temperature anisotropies of the form $1 - T_{\perp p}/T_{\|p} = S_p/\beta_{\|p}^{\alpha_p}$ where $\beta_{\|p} \equiv 8\pi n_p k_B T_{\|p}/B_\circ^2$, and the fitting parameters $S_p \sim 1$ and $\alpha_p \simeq 0.7$. Observations from the Wind spacecraft are reported here. These measurements show for the first time with a comprehensive plasma and magnetic field data set that this constraint is statistically satisfied in the solar wind near 1 AU, with best-fit values of $S_p = 1.21 \pm 0.26$ and $\alpha_p = 0.76 \pm 0.14$. *INDEX TERMS:* 7871 Space Plasma Physics: Waves and instabilities; 7867 Space Plasma Physics: Wave/particle interactions; 2164 Interplanetary Physics: Solar wind plasma. **Citation:** Kasper, J. C., A. J. Lazarus, and S. P. Gary, Wind/SWE observations of firehose constraint on solar wind proton temperature anisotropy, *Geophys. Res. Lett.*, *29*(17), 1839, doi:10.1029/2002GL015128, 2002.

1. Introduction

[2] We have analyzed solar wind proton temperature anisotropies observed by the two Faraday Cup (FC) instruments of the Solar Wind Experiment (SWE) on the Wind satellite [*Ogilvie et al.*, 1995]. Using more than seven years of data we demonstrate that the observed limit to the proton temperature anisotropy for $T_{\|p}/T_{\perp p} > 0$ is in agreement with the constraint which theory and simulations predict should be imposed by the firehose instability. Knowledge of the proton temperature anisotropy is sufficient for probing the firehose instability - discussed in detail in the following section - because electrons are nonresonant and the contribution due to alpha particles and other minor ions may be neglected to first order.

[3] This constraint from the firehose instability is analogous to a similar temperature anisotropy constraint which has been obtained by theoretical and computational methods for the electromagnetic proton cyclotron anisotropy instability driven by $T_{\perp p}/T_{\|p} > 1$ [see *Gary et al.*, 2000, and references therein]. This latter constraint has been verified through observations in the magnetosheath [*Phan et al.*, 1994; *Anderson et al.*, 1994; *Tan et al.*, 1998], in the outer magnetosphere [*Anderson et al.*, 1996], in the solar wind [*Gary et al.*, 2001] and in a laboratory experiment [*Scime et al.*, 2000]. In contrast, the only previous observational study of the temperature anisotropy constraint imposed by the firehose instability has been the work of *Eviatar and Schulz* [1970] who assumed a constant magnetic field for a limited data set of several hours measured by the Vela 4 spacecraft.

[4] Since this is the first time ion temperature anisotropies have been measured with SWE, we first present an outline of the technique and review its success before describing the theoretical predictions and our observations.

[5] A Faraday Cup is an energy/charge instrument with a large, conical field of view ($\sim$45° half-angle) which measures the current produced by particles within a given energy window. Due to the large acceptance angle of the FC, this current is proportional to the reduced distribution function, i.e. the ion distribution in velocity space integrated over all velocities perpendicular to the instrument axis.

[6] Wind is a rotating spacecraft with a spin-axis perpendicular to the ecliptic plane and a period of three seconds. The two FC instruments on Wind are mounted ±15° out of the ecliptic. Defining θ as the Sun-instrument angle in the plane of the ecltiptic, each FC makes measurements along 20 values of θ bracketing the solar wind flow during each rotation. Typically a complete spectrum includes measurements over 31 energy windows centered on the peak energy of the solar wind protons. We convolve the currents measured along the combination of energy windows and angles with an analytic expression for the response of the FC to a given velocity distribution. A non-linear least-squares χ^2 minimization routine yields the best fit parameters and their uncertainties.

[7] The simultaneous characterization of solar wind proton and alpha particles by the FC instruments on Wind as isotropic, convected Maxwellians has been described elsewhere [*Aellig et al.*, 2001; *Steinberg et al.*, 1996]. In the case of an ion of charge q described by a convected isotropic Maxwellian with a bulk velocity $\vec{U}$, number density n and thermal speed w, a FC performing a measurement in a speed window of v and $v + \Delta v$ will observe a current, I_{iso}, given by

$$I_{iso}(w) = \frac{Anq}{\pi^{3/2} w^3} \int_v^{v+\Delta v} \vec{v} \cdot \hat{n} e^{-\left(\vec{v}-\vec{U}\right)^2/w^2} d^3v, \qquad (1)$$

where A is the effective area of the collector and $\hat{n}$ is the direction the FC is pointing. If a two-temperature anisotropy

0094-8276/02/2002GL015128$05.00

exists with corresponding thermal speeds $w_{\|}$ and $w_{\perp}$ parallel and perpendicular to the magnetic field, then it can be shown that the observed current I_{ani} is given by $I_{ani} = I_{iso}(\tilde{w})$, where $\tilde{w}$ is an effective thermal speed which is a function of the orientation between the FC and the ambient magnetic field. With $\hat{b} \equiv \vec{B}/|\vec{B}|$, $\tilde{w}$ is given by

$$\tilde{w} = \sqrt{w_{\|}^2\left(\hat{n}\cdot\hat{b}\right)^2 + w_{\perp}^2\left(1-\left(\hat{n}\cdot\hat{b}\right)^2\right)}. \quad (2)$$

The simplicity of this response to a bi-Maxwellian distribution is due to the fact that a FC measures the reduced distribution function and has a very flat angular response.

2. Predicted Limit to Anisotropy

[8] If the proton velocity distribution in a collisionless electron/proton plasma is approximately bi-Maxwellian and bears the temperature anisotropy $T_{\|p} > T_{\perp p}$, then the proton firehose instability may arise. This growing mode has a real frequency ω_r which satisfies $\omega_r < \Omega_p$ where Ω_p is the proton cyclotron frequency. *Gary et al.* [1998] showed that under resonant conditions the linear threshold condition for a fixed value of the dimensionless maximum growth rate γ_m/Ω_p of this instability in an electron-proton plasma can be written for $\gamma_m/\Omega_p \leq 0.10$ as

$$1 - \frac{T_{\perp p}}{T_{\|p}} = \frac{S_p}{\beta_{\|p}^{\alpha_p}} \equiv R \quad (3)$$

over $1 \lesssim \beta_{\|p} \leq 10$ where $\beta_{\|p} \equiv 8\pi n_p k_B T_{\|p}/B_o^2$ (n_p is the proton number density, and k_B is Boltzmann's constant), S_p and α_p are fitting parameters; the former is a dimensionless number of order unity determined by the choice of maximum growth rate, but $\alpha_p \simeq 0.7$, relatively independent of γ_m/Ω_p. In the nonresonant long-wavelength limit, the firehose instability threshold corresponds to $S_p = 2$ and $\alpha_p = 1$.

[9] *Gary et al.* [1998] have also carried out hybrid simulations of this instability using bi-Maxwellian initial proton velocity distributions and have demonstrated that this growing mode imposes an upper bound on the proton temperature anisotropy of the form of equation (3). Their interpretation is that, if the anisotropy exceeds the instability threshold, the resulting enhanced fluctuations scatter the protons so as to reduce $T_{\|p}/T_{\perp p}$ back to and below that threshold. Their one-dimensional simulations suggest that the anisotropy constraint corresponds to $S_p = 1.5$ and $\alpha_p = 0.74$, whereas their two-dimensional simulations yield an upper bound corresponding to $S_p = 2.0$ and $\alpha_p = 1.0$, which is the nonresonant firehose instability threshold.

3. Wind Observations

[10] For this analysis, three-second magnetic field measurements provided by the Magnetic Field Experiment (MFI) on Wind are averaged over the duration of each FC spectrum. The average direction of the field determines $\hat{b}$ for subsequent fitting of the data with the anisotropic response function. Examination of the angular fluctuation of the field measurements indicates that the determination of the anisotropy is hindered when this fluctuation exceeds 20°. In subsequent analysis spectra with angular fluctuations of more than 15° are discarded.

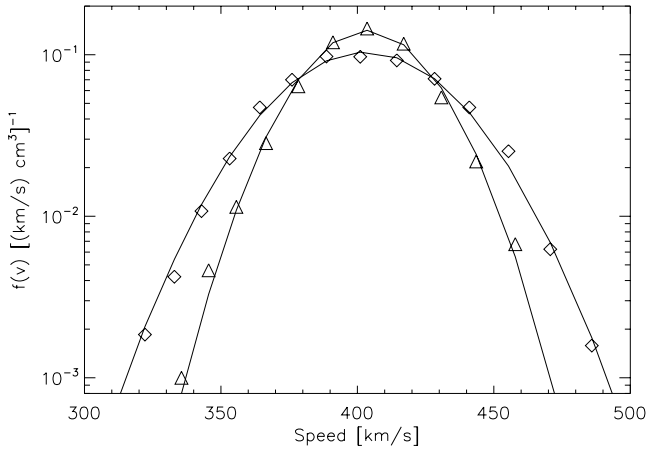

Figure 1. Reduced solar wind proton distribution function from a spectrum recorded by SWE at 3:3:34 [UT] on September 17, 2000. Symbols are observations for two angles relative to the magnetic field: 38° (diamonds) and 80° (triangles); curves are the best fit to the protons of a bi-Maxwellian yielding thermal speeds $w_{\|} = 46.6 \pm 4.1$, $w_{\perp} = 29.0 \pm 1.3$ [km/s].

[11] Figure 1 is a plot comparing measurements to the best fit model results for a single spectrum taken on September 17, 2000. Only two measurement angles of the total 40 are shown in this plot. Note the variation in thermal width of the proton distribution as the FC scans at different angles with respect to the magnetic field. Typically 200–300 measurements are selected in each spectrum to characterize the proton distribution.

[12] Over the course of the mission 1.9 million spectra taken in the solar wind were selected for this analysis. The average value of χ^2 per degree of freedom for these measurements is 1.12 ± 0.84, indicating that on average the core distributions of protons in the solar wind are well-described by two-temperature bi-Maxwellian distributions. In the case of proton double streaming, a frequent occurrence in the solar wind, only the properties of the core are used for this study. We feel this is justified because an independent study of SWE/FC observations of proton double streaming [D. Clack, private communication, 2002] shows that double streaming occurs rarely in the sub-set of data ($\beta_{\|p} \geq 1$, $T_{\|p}/T_{\perp p} > 0$) used to probe the firehose instability.

[13] The uncertainty in the thermal speeds is a function of the orientation of the magnetic field during each spectrum. For example, the uncertainty in $w_{\|}$ diverges rapidly as the field exceeds ±75° from the ecliptic plane. Fortunately the typical field direction along the Parker spiral at 1 A.U. results in the near minimum overall uncertainty in the two speeds. The average percent uncertainties in the thermal speeds are $\sigma_{w\perp} = (4.3 \pm 6.8)\%$ and $\sigma_{w\|} = (7.1 \pm 4.1)\%$.

[14] For each of the solar wind spectra we calculated the anisotropy ratio R as defined in equation (3) and estimated the uncertainty in the ratio, σ_R, by propagating the uncer-

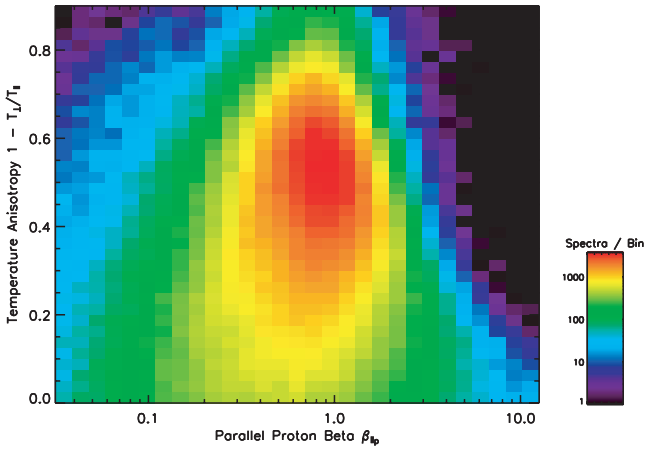

Figure 2. Two-dimensional histogram of all solar wind spectra with $T_{\|p} > T_{\perp p}$ as a function of parallel plasma beta $\beta_{\|p}$ and anisotropy ratio R. Color shading is logarithmic in the number of spectra per bin.

tainties in the individual thermal speeds from the best fit results. Data were selected for the final analysis by requiring $\sigma_R < 0.2$ and χ^2 per degree of freedom (d.o.f.) <5. A detailed examination of spectra with large values of χ^2/d.o.f. indicates that the existence of high energy tails or double streaming of the protons leads to a poor model fit. We discarded those measurements since the theoretical calculations of the firehose limit assume the distribution is bi-Maxwellian. Overall 32% or 0.6 million measurements met these cuts and had values of $0 \leq R \leq 1$ ($T_{\|p}/T_{\perp p} > 1$).

[15] In Figure 2 we have created a two-dimensional histogram of the number of spectra as a function of R and $\beta_{\|p}$. Figure 2 clearly demonstrates that the proton temperature anisotropy is more strongly constrained as $\beta_{\|p}$ increases, and that this type of constraint corresponds only to $\beta_{\|p} \geq 1$. These qualities are both hallmarks of equation (3) and represent strong evidence that this constraint is due to the proton firehose instability.

[16] To quantify the observed limit for comparison with predictions, we calculated a critical value, R_c, of the anisotropy ratio as a function of $\beta_{\|p}$ for comparison with the predicted threshold condition. Observations were divided into 30 bins in $\beta_{\|p}$, with constant logarithmic spacing as indicated by the pixel sizes in Figure 2. The number of spectra seen as a function of R for fixed $\beta_{\|p}$ falls off exponentially with increasing R. We fit this fall off with an exponential curve, as shown in Figure 3 for four intervals of $\beta_{\|p}$, and define R_c as the value of R where the number of spectra fell to 10% of its maximum value. The parameters and their uncertainties for the best fit exponential curve are then used to determine R_c and its uncertainty σ_{Rc}.

[17] The results of this study are summarized in Figure 4. To better visualize the dependence of R_c on $\beta_{\|p}$ we have taken the two-dimensional histogram from Figure 2 and normalized each column of bins of a given $\beta_{\|p}$ to unity by the bin in that column with the maximum number of spectra. The red crosses are values of R_c determined by fitting the fall off in the number of spectra, with horizontal error bars marking the width of each bin in $\beta_{\|p}$ and vertical error bars indicating σ_{Rc}. Values of R_c with over-plotted diamonds ($2 \leq \beta_{\|p} \leq 20$) were selected for fitting to equation (3), yielding best fit values of $S_p = 1.21 \pm 0.26$ and $\alpha_p = 0.76 \pm 0.14$.

[18] This fit to the observed constraint on the proton temperature anisotropy is in very good agreement with both the linear theory of the resonant firehose instability and the 1-D simulation results of *Gary et al.* [1998], which also yielded $\alpha_p \simeq 0.74$ on the range $2 \leq \beta_{\|p} \leq 10$. There is less good agreement with the linear theory of the nonresonant firehose instability and the 2-D simulations of *Gary et al.* [1998] which indicate $\alpha_p = 1.0$. We conclude that, over $2 \leq \beta_{\|p} \leq 10$, our observations are consistent with the imposition of an upper bound on the proton temperature anisotropy by wave-particle scattering due to enhanced fluctuations from the proton firehose instability. Furthermore, our observations indicate that it is the proton-resonant firehose which is the more likely source of the fluctuations which lead to this constraint.

[19] The firehose instability based on a bi-Maxwellian proton velocity distribution is essentially stable at $\beta_{\|p} \leq 1$, and cannot be responsible for the apparent decrease in the average anisotropy as $\beta_{\|p}$ decreases from unity. It may be that this feature corresponds to the proton-proton Alfvén instability which has a lower effective $T_{\|}$ at threshold as β_p decreases [e.g., see Figure 1 of *Montgomery et al.*, 1976].

4. Conclusions

[20] The Faraday Cup instruments on Wind have been used to accurately measure ion temperature anisotropies. By using a non-linear fitting routine to characterize the spectra we obtain uncertainties and χ^2 in addition to the best fit parameters. We have used a comprehensive plasma and magnetic field dataset from Wind to show for the first time that the theoretical threshold of the firehose instability provides a statistical upper bound on $T_{\|p}/T_{\perp p}$ values observed at $\beta_{\|p} \geq 2$ in the solar wind. The observed limit

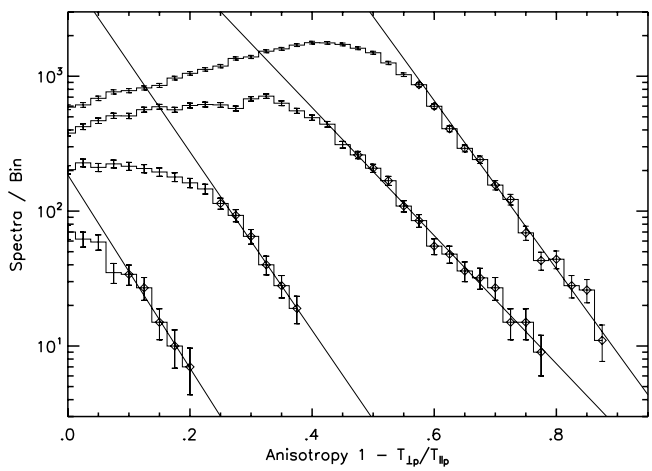

Figure 3. Histograms of number of spectra as a function of anisotropy for four bins in $\beta_{\|p}$. From top to bottom the average value of $\beta_{\|p}$ in each bin is: 1.3, 2.0, 3.5, 10.0. Error bars are statistical uncertainty, diamonds are points selected for fitting, and lines are the best fit exponential.

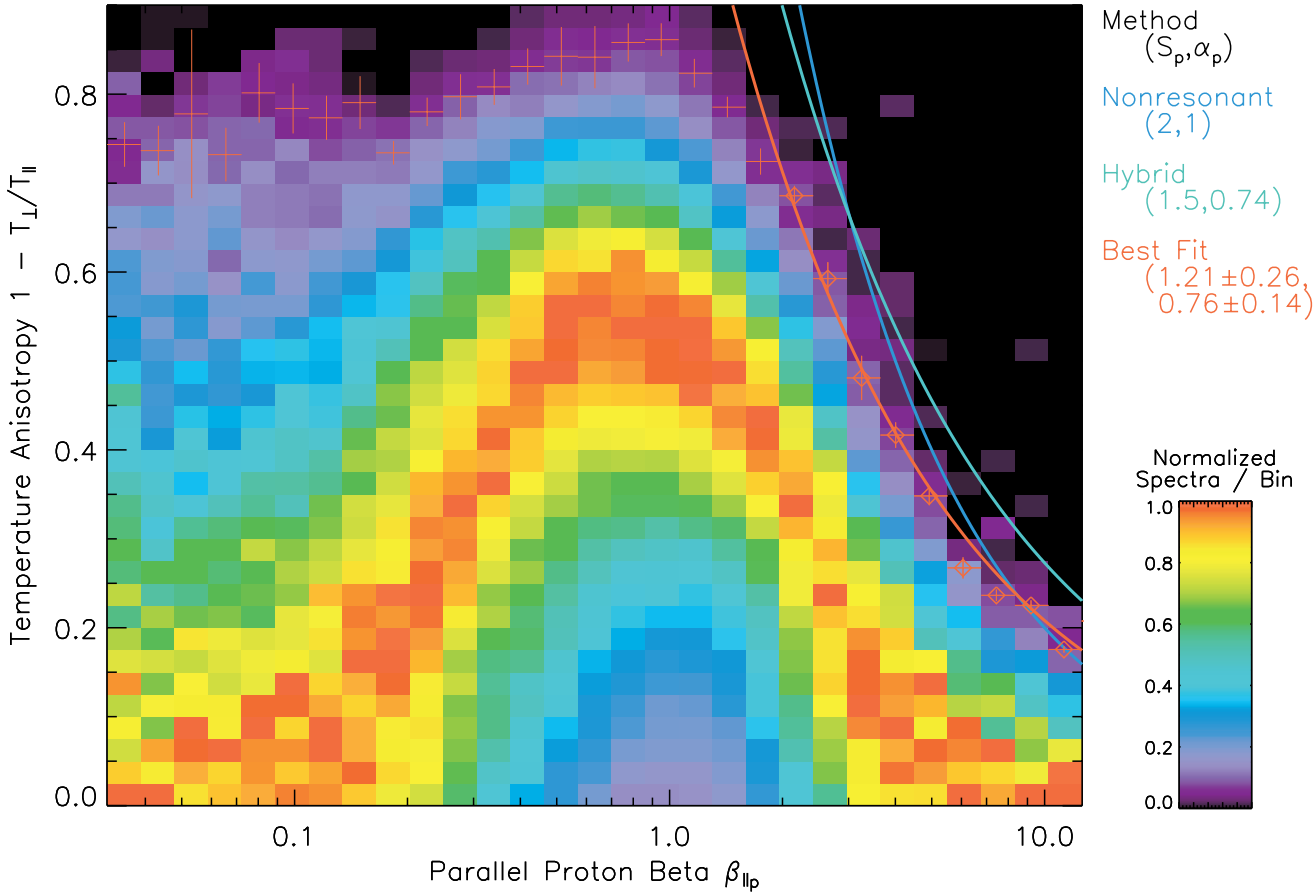

Figure 4. Two-dimensional histogram of the measurements with each column in $\beta_{\|p}$ normalized to unity by the maximum number of spectra in a single bin in that column. Color scale is linear. Red crosses are R_c at given values of $\beta_{\|p}$ with the horizontal error bars indicating the width of the bin and vertical error bars one σ uncertainty in R_c. Red diamonds are values of R_c at $\beta_{\|p} \geq 2$ selected for fitting with equation (3). Curves are nonresonant limit (blue), limit from one-dimensional hybrid simulation (green) and best fit to data (red).

in R for $\beta_{\|p} < 1$ merits further study, possibly by using a model proton velocity distribution which allows departures from a bi-Maxwellian.

[21] **Acknowledgments.** J. Kasper and A. Lazarus thank James Tanabe for his assistance in verifying the anisotropic analysis method for Faraday Cups and A. Szabo from the Wind/MFI experiment for the magnetic field data. This work was supported in part by NASA grant NAG-10915. The Los Alamos portion of this work was done under the auspices of the US Department of Energy, and was supported by both DOE and NASA programs.

References

Aellig, M. R., A. J. Lazarus, and J. T. Steinberg, The solar wind helium abundance: Variation with wind speed and the solar cycle, *Geophys. Res. Lett.*, *28*, 2767, 2001.

Anderson, B. J., S. A. Fuselier, S. P. Gary, and R. E. Denton, Magnetic spectral signatures in the Earth's magnetosheath and plasma depletion layer, *J. Geophys. Res.*, *99*, 5877, 1994.

Anderson, B. J., R. E. Denton, G. Ho, D. C. Hamilton, S. A. Fuselier, and R. J. Strangeway, Observational test of local proton cyclotron instability in the Earth's magnetosphere, *J. Geophys. Res.*, *101*, 21,527, 1996.

Eviatar, A., and M. Schulz, Ion-temperature anisotropies and the structure of the solar wind, *Planet. Space Sci.*, *18*, 321, 1970.

Gary, S. P., H. Li, S. O'Rourke, and D. Winske, Proton resonant firehose instability: Temperature anisotropy and fluctuating field constraints, *J. Geophys. Res.*, *103*, 14,567, 1998.

Gary, S. P., L. Yin, and D. Winske, Electromagnetic proton cyclotron anisotropy instability: Wave-particle scattering rate, *Geophys. Res. Lett.*, *27*, 2457, 2000.

Gary, S. P., R. M. Skoug, J. T. Steinberg, and C. W. Smith, Proton temperature anisotropy constraint in the solar wind: ACE observations, *Geophys. Res. Lett.*, *28*, 2759, 2001.

Montgomery, M. D., S. P. Gary, W. C. Feldman, and D. W. Forslund, Electromagnetic instabilities driven by unequal proton beams in the solar wind, *J. Geophys. Res.*, *81*, 2743, 1976.

Ogilvie, K. W., et al., SWE, A comprehensive plasma instrument for the Wind spacecraft, *Space Science Reviews*, *71*, 55–77, 1995.

Phan, T.-D., G. Paschmann, W. Baumjohann, N. Sckopke, and H. Lühr, The magnetosheath region adjacent to the dayside magnetopause: AMPTE/IRM observations, *J. Geophys. Res.*, *99*, 121, 1994.

Scime, E. E., P. A. Keiter, M. M. Balkey, R. F. Boivin, J. L. Kline, M. Blackburn, and S. P. Gary, Ion temperature anisotropy limitation in high beta plasmas, *Phys. Plasmas*, *7*, 2157, 2000.

Steinberg, J. T., A. J. Lazarus, K. W. Ogilvie, R. Lepping, and J. Byrnes, Differential flow between solar wind protons and alpha particles: First Wind observations, *Geophys. Res. Lett.*, *23*, 1183–1186, 1996.

Tan, L. C., S. F. Fung, R. L. Kessel, S.-H. Chen, J. L. Green, and T. E. Eastman, Ion temperature anisotropies in the Earth's high-latitude magnetosheath: Hawkeye observations, *Geophys. Res. Lett.*, *25*, 587, 1998.

J. C. Kasper and A. J. Lazarus, Center for Space Research, Massachusetts Institute of Technology, 77 Massachusetts Avenue, Cambridge, MA 02139, USA. (jck@space.mit.edu; ajl@space.mit.edu)

S. P. Gary, M.S. D466, Los Alamos National Laboratory, Los Alamos, NM 87545, USA. (pgary@lanl.gov)